CODEN STJSAO
ZX470/1436

ISSN 0562-1887
UDK 537.874:519.61:624.073.8

Dynamic Nonlinear Temperature Field in a Ferromagnetic Plate Induced by High Frequency Electromagnetic Waves

***Vesna MILOŠEVIĆ MITIĆ*[1)], *Dražan KOZAK*[2)], *Taško MANESKI*[1)], *Nina ANĐELIĆ*[1)], *Branka GAĆEŠA*[1)] and *Marinko STOJKOV*[2)]**

1) Mašinski fakultet Univerziteta u Beogradu, (Faculty of Mechanical Engineering, University of Belgrade), Kraljice Marije 16, 11120 Beograd, **Republic of Serbia**

2) Strojarski fakultet u Slavonskom Brodu, Sveučilišta J. J. Strossmayera u Osijeku (Mechanical Engineering Faculty, J. J. Strossmayer University of Osijek), Trg Ivane Brlić-Mažuranić 2, HR-35000 Slavonski Brod, **Republic of Croatia**

vmilosevic@mas.bg.ac.rs

Keywords

Electromagnetic field
Ferromagnetic plate
High frequency wave
Temperature

Ključne riječi

Elektromagnetno polje
Feromagnetska ploča
Temperatura
Visokofrekventni val

Received (primljeno): 2009-09-01
Accepted (prihvaćeno): 2010-02-19

Original scientific paper

The subject of this paper is the thermal-behavior of an elastic metallic plate influenced by several harmonic electromagnetic plane waves at the upper and lower surfaces. The direction of wave propagation is normal to the surfaces of the plate. As a result of a time-varying electromagnetic field conducting currents appear in the plate. Distributions of eddy-currents and hysterisis power losses across the plate thickness are obtained using complex analysis. It is of the exponential type and depends on the plate thickness, wave frequency, electric conductivity, magnetic permeability and magnetic intensity. By treating this power as a volume heat source, differential equations governing distribution of the temperature field are formulated. The temperature field across the plate thickness is assumed to be in nonlinear form and a system of three coupled differential equations governing the temperature field is formed. Equations are solved in analytical form using the integral-transformation technique (Double Fourier finite-sine transformation and Laplace transformation). The influence of the skin depth, plate thickness, wave frequency and characteristic times of an impulse on the dynamic temperature field are considered. Nonlinear distribution of the temperature across the plate thickness is obtained. Strain and stress fields are obtained using the finite element method (FEM). Depending on the plate thickness thin shell finite elements (for a thin plate) or volume finite elements (for a thick plate) were applied.

Dinamičko nelinearno polje temperature u feromagnetskoj ploči induciranoj visokofrekventnim valovima

Izvornoznanstveni članak

Tema ovog rada je toplinsko ponašanje tanke feromagnetske elastične ploče inducirane većim brojem ravninskih harmonijskih elektromagnetskih valova na gornjoj i na donjoj površini. Pravac prostiranja valova je okomit na srednju ravninu ploče. Kao rezultat vremenski promjenljivog elektromagnetskog polja u ploči se pojavljuju inducirane struje. Raspodjela toplinskih gubitaka po debljini ploče uslijed induciranih struja i histereze određena je primjenom složenog proračuna. Ona je eksponencijalnog tipa i ovisi o debljini ploče, frekvenciji valova, električnoj vodljivosti materijala, magnetskoj permeabilnosti i magnetskoj indukciji. Tretiranjem snage toplinskih gubitaka kao volumnog izvora topline, formirane su diferencijalne jednadžbe koje opisuju raspodjelu polja temperature u ploči. Temperaturno polje po debljini ploče definirano je u nelinearnom obliku i dobivene su tri spregnute diferencijalne jednadžbe. Jednadžbe su riješene u analitičkom obliku primjenom tehnike integralnih transformacija (Dvostruka Fourierova konačna-sinus transformacija i Laplaceova transformacija). Razmatran je i vremenski utjecaj dubine prodiranja valova, debljine ploče, frekvencije valova i perioda impulsa na polje temperature. Određena je nelinearna raspodjela polja temperature po debljini ploče. Polja naprezanja i deformacija dobivene su primjenom metode konačnih elemenata. U ovisnosti o debljini ploče primjenjivani su konačni elementi tanke ljuske i volumni konačni elementi.

Symbols/Oznake

B	- magnetic induction, T - magnetska indukcija
D	- electric induction, C/m^2 - električna indukcija
H	- intensity of the magnetic field, A/m - intenzitet magnetnog polja
K	- intensity of the electric field, V/m - intenzitet električnog polja
J	- current density, A/m^2 - gustoća struje
P	- density of the power of heat losses, W/m^3 - gustoća snage toplinskih gubitaka
W	- heat source intensity, W/m^3 - intenzitet izvora topline
T_0	- temperature of the plate in its natural state, K - temperatura ploče u prirodnom stanju
θ	- temperature field, $\theta = T\text{-}T_0$, K - temperaturno polje
μ	- magnetic permeability, H/m - magnetska permeabilnost
σ	- electric conductivity, S/m - električna provodljivost
ε_0	- dielectric constant of vacuum, F/m - dielektrična konstanta vakuuma
κ	- coefficient of thermal intensity, m^2/s - koeficijent termičke difuzije
λ_0	- heat conduction coefficient, W/(m·K) - koeficijent toplinske vodljivosti
δ	- skin depth, m - dubina prodiranja vala
a, b	- plate dimensions, m - dimenzije ploče u srednjoj ravnini
h	- plate thickness, m - debljina ploče
f	- wave frequency, Hz - frekvencija vala
ω	- wave angular frequency, rad/s - kutna frekvencija vala
k_H	- hysterisis factor - faktor histereze
t	- time, s - vrijeme
t_{oi}	- the moment of wave occurrence, s - vrijeme pojave vala
t_{Ii}	- the moment of wave disappearance, s - vrijeme nestanka vala
∂_t	- time derivative - vremenska derivacija
$H(t)$	- Heaviside function - Heavisideova funkcija
∇_1^2	- two-dimension Laplace operator - dvodimenzijski Laplaceov operator

1. Introduction

The theory of electro-magneto-thermoelasticity investigates interactions between strain and the electromagnetic field in a solid elastic body. It has received considerable attention because of possible applications in the detection of flaws in ferrous metals, optical acoustics, levitation by superconductors, magnetic fusion. As a special scientific field, electro-magneto-thermoelasticity started developing at the end of the fifties and first applications were in geophysics and some branches of acoustics.

Propagation of an elastic field in the presence of a magnetic field was considered by L. Knopoff (1955), J.W. Dunkin and A.C. Eringen (1963). F.W. Brown (1966) developed a rigorous phenomenological theory for ferromagnetic materials on the basis of the large deformation theory and the classical theory of ferromagnetism. H.F. Tiersten (1964) developed an analogous theory based on a microscopic model. Since the general nonlinear theory is complicated, Y.W. Pao and C.S. Yeh [1] derived a set of linear equations and boundary conditions for soft ferromagnetic elastic materials. They applied the linear theory to investigate magnetoelastic buckling of an isotropic plate. The same problem was treated in another way by F.C. Moon and Y.H. Pao [2]. This theory was applied by Y. Shindo [3] to define the intensification factors of cracks in ferromagnetic elastic solids. S.K. Roychoudhuri, L. Debnath, M. Banerjee [4, 5] considered the influence of magnetic fields in a rotating media.

The basic general information about the theory of magneto-thermoelasticity was presented in the monograph by H. Parkus [6]. A great contribution to research in

this scientific field was given by W. Nowacki, S.A. Ambarcumian (1977), M. Krakowski [7]. In 1975 a set of experiments was done at the Michigan Technological University (N.S. Christopherson, M.O. Peach, J.M. Dalrymple, L.G. Viegelahn [8]), to reconsider theoretical results. Because of a disagreement in analytical and experimental results methods of numerical analyses were involved (K. Miya, T. Takagi, Y. Ando (1980), X. Tian and Y. Shen (2006)). A mathematical model for the temperature field developed during high frequency induction heating was established by Shen, Yao, Shi and Hu [9]. Sharma and Pal investigated propagation of the magnetic-thermoelastic plane wave in a homogeneous isotropic conducting plate under a uniform static magnetic field (2004). The two-dimensional problem of electro-magneto-thermoelasticity for a perfectly conducting thick plate subjected to a time dependent heat source was studied by Allam, Elsibai and Abouelregal (2009). A model calculation of high temperature superconducting microstrip transmission lines was performed by V. A. Krakovskii [10].

2. Basic equations

The electro-magneto-thermoelastic problem considered in this paper shows one type of interaction between electromagnetic, temperature and strain fields in a solid plate. It is assumed that the plate material is elastic, isotropic, soft ferromagnetic, and has good electric conductivity. Many nickel-iron alloys used for building the magnetic circuits of motors, generators, inductors, transformers are of this type.

As a result of a time changing electromagnetic field conducting currents appear in electric conductors. This problem is mathematically described by a system of Maxwell's equations with relations for slowly moving media and modified Ohm's law [6]

$$\begin{aligned} &rot\vec{H} = \vec{J} + \frac{\partial \vec{D}}{\partial t} \qquad rot\vec{K} = -\frac{\partial \vec{B}}{\partial t} \\ &div\vec{D} = 0 \qquad div\vec{B} = 0 \\ &\vec{D} = \varepsilon_0\left(\vec{K} + \dot{\vec{u}} \times \vec{B}\right) \qquad \vec{B} = \mu\left(\vec{H} - \dot{\vec{u}} \times \vec{D}\right) \\ &\vec{J} = \sigma\left(\vec{K} + \dot{\vec{u}} \times \vec{B}\right), \end{aligned} \tag{1}$$

where the following notation is applied: H – intensity of the magnetic field, K – intensity of the electric field, B – magnetic flux density (magnetic induction), D – electric induction, J – current density, u – deflection, μ – magnetic permeability, σ - electric conductivity, ε_0 – dielectric constant of vacuum, t –time.

The power of the conducting currents is represented by one type of volume heat source in the plate. So, the system of equations describing the temperature field in a plate is [11]

$$\begin{aligned} &\left(\nabla^2 - \frac{1}{\kappa}\frac{\partial}{\partial t}\right)\theta - \eta\, \dot{u}_{j,j} = -\frac{W}{\lambda_0}, \\ &W = W_E + W_H + \frac{J^2}{\sigma},\ (j = 1,2,3) \end{aligned} \tag{2}$$

where κ is the coefficient of thermal intensity, η is the coupling between the temperature and the deformation fields, λ_0 is the heat conduction coefficient, ∇^2 is the Laplace operator and ∂_t is the time derivative. The temperature field is presented as θ [°C, K] = T-T_0 where T_0 is the temperature of the plate in its natural state.

The quantity of heat generated in a unite volume and unit time (heat source intensity) $W(x_1, x_2, x_3, t)$ consists of three parts: intensity of external heat source W_E, hysterisis losses W_H and Joule's heat (eddy-current losses).

We can make the assumption that the temperature changes are nonlinear across the thickness of the plate. Using the Cartesian coordinate system presented on Figure 1, the temperature field θ (x_1, x_2, x_3, t) can be described using three values, τ_0, τ_1 and τ_2 as

$$\begin{aligned} &\theta(x_1, x_2, x_3, t) = \tau_0(x_1, x_2, t) + x_3\tau_1(x_1, x_2, t) + \\ &+ x_3^2\tau_2(x_1, x_2, t). \end{aligned} \tag{3}$$

If we multiply equation (2) with x_3^k (k=0,1,2) and make an integration from the plate thickness, we obtain three partial differential equations describing the temperature field in a plate [12]

$$\begin{aligned} &\left(\nabla_1^2 - \frac{1}{\kappa}\frac{\partial}{\partial t}\right)\left(\tau_0 + \frac{h^2}{12}\tau_2\right) + \frac{1}{h}\left[\frac{\partial\theta}{\partial x_3}\right]_{-\frac{h}{2}}^{\frac{h}{2}} = -\frac{W_0}{h\,\lambda_0}, \\ &\left(\nabla_1^2 - \frac{12}{h^2} - \frac{1}{\kappa}\frac{\partial}{\partial t}\right)\tau_1 + \frac{12}{h^3}\left[x_3\frac{\partial\theta}{\partial x_3}\right]_{-\frac{h}{2}}^{\frac{h}{2}} = -\frac{12W_1}{h^3\lambda_0}, \\ &\left(\nabla_1^2 - \frac{1}{\kappa}\frac{\partial}{\partial t}\right)\left(\tau_0 + \frac{3h^2}{20}\tau_2\right) - 4\tau_2 + \frac{12}{h^3}\left[x_3^2\frac{\partial\theta}{\partial x_3}\right]_{-\frac{h}{2}}^{\frac{h}{2}} = \\ &= -\frac{12W_2}{h^3\lambda_0}, \\ &W_k = \int_{-\frac{h}{2}}^{\frac{h}{2}} W(x_1, x_2, x_3, t)\, x_3^k\, dx_3,\ (i = 0,1,2) \end{aligned} \tag{4}$$

where h is the plate thickness and ∇_1^2 is the two-dimension Laplace operator: $\nabla_1^2 = \frac{\partial^2}{\partial x_1^2} + \frac{\partial^2}{\partial x_2^2}$..

Of course, the presented system of equations has to be completed with an appropriate set of boundary and initial conditions.

In taking into account plate vibrations, we shall involve finite element analysis together with the analytically obtained solutions.

3. Conducting currents. Joule's heat. Hysterisis losses

An electromagnetic wave with complex time-varying fields can be represented as a sum of simple plane waves. So, first we have to determine the analytical expression for the power of one harmonic plane wave with K_0 and H_0 components on the upper surface of the plate. It is assumed that all field components vary in time t as exp$(j\omega t)$, where ω is the appropriate angular frequency.

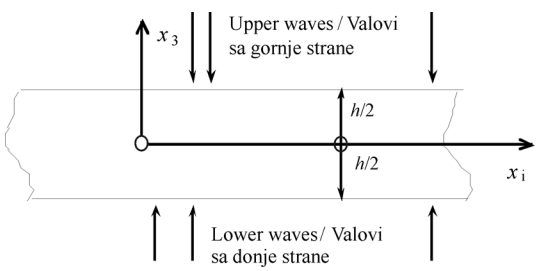

Figure 1. Coordinate system (middle surface of the plate)
Slika 1. Koordinatni sustav (srednja ravnina ploče)

In the case of high plate conductivity, the dielectric current can be neglected in comparison with the conducting current. So, for a homogeneous, isotropic and linear magnetic medium the system of Maxwell's equations (1) can be presented in the form [13]

$$\begin{aligned} &rot\vec{H} = \sigma\vec{K}, && div\vec{K} = 0, \\ &rot\vec{K} = -\mu\frac{\partial\vec{H}}{\partial t}, && div\vec{H} = 0. \end{aligned} \tag{5}$$

Using the symbolic-complex method ($\vec{A} = \underline{\vec{A}}e^{j\omega t}$) we obtain the following equations

$$\begin{aligned} &rot\underline{\vec{H}} = \sigma\underline{\vec{K}}, && div\underline{\vec{K}} = 0, \\ &rot\underline{\vec{K}} = -\mu(j\omega)\underline{\vec{H}}, && div\underline{\vec{H}} = 0. \end{aligned} \tag{6}$$

If the direction of wave propagation is x_3-axe (negative) and if the field components are independent of x_1 and x_2, from the equations of divergence we can conclude that the components $\underline{H}_3$ and $\underline{K}_3$ are zero. In the case of a plane wave, only normal components of the electric and magnetic field depend on each other [11]. So, we will conduct the analysis only for one wave with components $\underline{K}_1$ and $\underline{H}_2$. Let them have the following values in plane $x_3=h/2$

$$\vec{K} = K_1\vec{i} = K_0\cos(\omega t)\vec{i}^{\circ}, \quad \vec{H} = H_2\vec{j} = H_0\cos(\omega t)\vec{j},$$
$$H_0 = \sqrt{\frac{\varepsilon}{\mu}}K_0 \tag{7}$$

Maxwell's equations (6) have the following form

$$-\frac{\partial\underline{H}_2}{\partial x_3} = \sigma\underline{K}_1, \quad \frac{\partial\underline{K}_1}{\partial x_3} = -\mu j\omega\underline{H}_2$$

or

$$\frac{\partial^2\underline{H}_2}{\partial x_3^2} - \gamma\underline{H}_2 = 0, \quad \underline{K}_1 = -\frac{1}{\sigma}\frac{\partial\underline{H}_2}{\partial x_3}, \tag{8}$$

where

$\gamma^2 = j\sigma\mu\omega$, $\gamma=\alpha+j\beta$, $\alpha = \beta = \sqrt{\frac{\sigma\mu\omega}{2}}$.

The basic solution of equation (8) can be represented as

$$\underline{H}_2 = \underline{C}e^{\gamma x_3}, \quad \underline{K}_1 = \frac{\gamma}{\sigma}\underline{H}_2. \tag{9}$$

Using the boundary condition for $x_3 = h/2$ we have

$$\underline{C} = H_0 e^{-\gamma\frac{h}{2}}. \tag{10}$$

The obtained result for the field components has the form

$$\begin{aligned} &\underline{H}_2 = H_0 e^{-\alpha h/2}e^{-j\beta h/2}e^{\alpha x_3}e^{j\beta x_3}, \\ &\underline{K}_1 = H_0\sqrt{\frac{\omega\mu}{\sigma}}e^{j\frac{\pi}{4}}e^{-\alpha h/2}e^{-j\beta h/2}e^{\alpha x_3}e^{j\beta x_3} \end{aligned} \tag{11}$$

or

$$H_2 = Re\left[\underline{H}_2 e^{j\omega t}\right] = H_0 e^{\alpha(x_3-h/2)}\cos\left(\omega t + \beta x_3 - \beta\frac{h}{2}\right),$$
$$K_1 = Re\left[\underline{K}_1 e^{j\omega t}\right] = H_0\sqrt{\frac{\omega\mu}{\sigma}}e^{\alpha(x_3-h/2)}\times$$
$$\times\cos\left(\omega t + \beta x_3 - \beta\frac{h}{2} + \frac{\pi}{4}\right).$$

The electromagnetic wave (11) is followed with the conducting currents, density

$$\underline{J}_1 = \sigma\underline{K}_1 = H_0\sqrt{\omega\mu\sigma}e^{\alpha(x_3-h/2)}e^{j\beta(x_3-h/2)}e^{j\frac{\pi}{4}}. \tag{12}$$

The distribution of Joule's heat $P_v(x_3)$ can be obtained in the following way

$$\|J\|^2 = \underline{J}_x\underline{J}_x^* = H_0^2\sigma\omega\mu e^{2\alpha(x_3-h/2)},$$
$$P_v(x_3) = \frac{1}{2\sigma}\|J\|^2 = \frac{1}{2\sigma}\underline{J}_x\underline{J}_x^*. \tag{13}$$

Distribution of the power of eddy-currents across the plate thickness is

$$P_v(x_3) = \frac{1}{2}H_0^2\omega\mu e^{-h\sqrt{\frac{\sigma\mu\omega}{2}}}e^{x_3\sqrt{2\sigma\mu\omega}}. \tag{14}$$

In the case of a nonlinear magnetic material the factor which involves heat losses of the hysterisis loop needs to be added to the presented calculation. For most soft ferromagnetic materials the basic curve of magnetization is nearly linear. This fact proves that the middle value for permeability can be used in the calculation. Hysterisis losses are proportional to the square of field amplitude and frequency

$$P_{\mathrm{H}} \approx H^2 f, \quad P_{\mathrm{H}}\left(x_3\right) = k_{\mathrm{H}} \mu H_0^2 f e^{2\alpha\left(x_3 - h/2\right)},$$

which proves that their distribution is the same as the distribution of eddy-current losses. Coefficient k_H is the hysterisis factor (material characteristic obtained in a laboratory).

The density of the power of heat losses is approximately

$$P\left(x_3\right) = \frac{1}{2} H_0^2 \omega \mu e^{-h\sqrt{\frac{\sigma\mu\omega}{2}}} \left(1 + \frac{k_{\mathrm{H}}}{\pi}\right) e^{x_3\sqrt{2\sigma\mu\omega}}. \tag{15}$$

The previous expression shows that the heat source intensity increases in an exponential way through the plate thickness. The gradient of the exponential curve increases with the increase of wave frequency, permeability and electric conductivity of the material.

The phenomenon of the conducting current concentration on the surface, valid for conductors with very high electric conductivity and magnetic permeability is known as the skin effect.

Let us analyze the case when we have j different waves on the upper and l waves on the lower side of the plate. Using (15) the power of one wave (i) can be expressed as a function of time as follows

$$W_i\left(x_3, t\right) = P_i e^{\pm 2\alpha x_i} H(t - t_{oi}), \tag{16}$$
$$P_i = \frac{1}{2} H_{0i}^2 \omega_i \mu e^{-h\sqrt{\frac{\sigma\mu\omega_i}{2}}} \left(1 + \frac{k_{\mathrm{H}}}{\pi}\right),$$

where for the upper waves we have sign (+) and for the lover waves sign (-).

So, the power of the eddy-current and the hysterisis losses can be presented as a function of x_3 and t

$$W\left(x_3, t\right) = \sum_{i=1}^{j} P_i e^{2\alpha_i x_3} H(t - t_{oi}) + \sum_{i=1}^{l} P_i e^{-2\alpha_i x_3} H(t - t_{oi}), \tag{17}$$

where t_{oi} is the moment of wave occurrence. Wave occurrence is defined using the Heaviside function. In the case when waves occur at t_{oi} and disappear at t_{1i} the Heaviside function is replaced with a pulse function

$$\Pi\left[\frac{t - \frac{1}{2}\left(t_{oi} + t_{1i}\right)}{t_{1i} - t_{oi}}\right] = H\left(t - t_{oi}\right) - H\left(t - t_{1i}\right). \tag{18}$$

4. Temperature field in the plate

Let the rectangular plate dimensions $a \times b \times h$ (Figure 2) be isolated on the upper and the lower surface and the temperature along the lateral sides is equal to the initial temperature T_0 ($\theta = T - T_0 = 0$). The initial and the boundary conditions have the form

$$\theta\big|_{t=0} = 0, \quad \theta\big|_{x_1=0,a} = 0, \quad \theta\big|_{x_2=0,b} = 0, \quad \frac{\partial\theta}{\partial x_3}\bigg|_{x_3=\pm\frac{h}{2}} = 0. \tag{19}$$

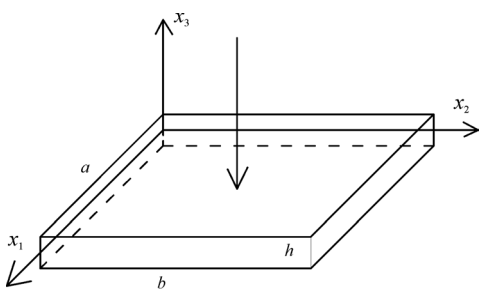

Figure 2. Rectangular plate $a \times b \times h$

Slika 2. Pravokutna ploča $a \times b \times h$

Subjected to the presented boundary conditions and relations (17), equation (4) can be represented in the following form

$$\left(\nabla_1^2 - \frac{12}{h^2} - \frac{1}{\kappa}\frac{\partial}{\partial t}\right)\tau_1 = -\frac{12 W_1}{h^3 \lambda_0},$$
$$\left(\nabla_1^2 - \frac{60}{h^2} - \frac{1}{\kappa}\frac{\partial}{\partial t}\right)\tau_2 = \frac{15}{h^3 \lambda_0}\left(W_0 - \frac{12}{h^2} W_2\right), \tag{20}$$
$$\left(\nabla_1^2 - \frac{1}{\kappa}\frac{\partial}{\partial t}\right)\left(\tau_0 + \frac{h^2}{12}\tau_2\right) = -\frac{W_0}{h\ \lambda_0},$$

where according to (4) we have

$$W_k = \begin{cases} \sum_{i=1}^{j+l} \frac{\mathrm{P_i}}{\alpha_i} Sh(\alpha_i h) H(t-t_{oi}), & \mathrm{k}=0 \\ \sum_{i=1}^{j} \frac{P_i}{2\alpha_i^2}\left[\alpha_i hCh(\alpha_i h) - Sh(\alpha_i h)\right] H(t-t_{oi}) - \sum_{i=1}^{l} \frac{P_i}{2\alpha_i^2}\left[\alpha_i hCh(\alpha_i h) - Sh(\alpha_i h)\right] H(t-t_{oi}), & \mathrm{k}=1 \\ \sum_{i=1}^{j+l} \frac{P_i}{4\alpha_i^3}\left[\left(\alpha_i^2 h^2 + 2\right) Sh(\alpha_i h) - 2\alpha_i hCh(\alpha_i h)\right] H(t-t_{oi}), & \mathrm{k}=2 \end{cases} \tag{21}$$

Equations (20) can be solved by using the integral- transformation technique.

Using notation

$$C_{ki} = \begin{cases} \frac{1}{h\lambda_0} \sum_{i=1}^{j+l} \frac{P_i}{\alpha_i} Sh(\alpha_i h) H(t-t_{oi}), & k=0 \\ \frac{12}{h^3\lambda_0} \frac{P_i}{2\alpha_i^2}\left[\alpha_i hCh(\alpha_i h) - Sh(\alpha_i h)\right], & k=1 \\ \frac{15}{h^3\lambda_0}\left(\frac{\mathrm{P_i}}{\alpha_i} Sh(\alpha_i h) - \frac{12}{h^2} \frac{P_i}{4\alpha_i^3}\left[\left(\alpha_i^2 h^2 + 2\right) Sh(\alpha_i h) - 2\alpha_i hCh(\alpha_i h)\right]\right), & k=2 \end{cases} \tag{22}$$

and applying the double Fourier finite-sine transformation (signed as *nm*) and the Laplace transformation (signed as **, $t \to p$*) we arrive to the transformation functions of the temperature field as

$$\tau_{kmn}^{*} = \begin{cases} \sum_{i=1}^{j+l} \frac{4C_{oi}\kappa}{\alpha_n\alpha_m} \frac{e^{-t_{oi}p}}{p\left(p+\kappa\Delta_{mn}\right)} + \frac{h^2}{12} \sum_{i=1}^{j+l} \frac{4C_{2i}\kappa}{\alpha_n\alpha_m} \frac{e^{-t_{oi}p}}{p\left[p+\kappa\left(\frac{60}{h^2}+\Delta_{mn}\right)\right]}, & k=0 \\ \sum_{i=1}^{j} \frac{4C_{ki}\kappa}{\alpha_n\alpha_m} \frac{e^{-t_{oi}p}}{p\left[p+\kappa\left(\frac{12}{h^2}+\Delta_{mn}\right)\right]} - \sum_{i=1}^{l} \frac{4C_{ki}\kappa}{\alpha_n\alpha_m} \frac{e^{-t_{oi}p}}{p\left[p+\kappa\left(\frac{12}{h^2}+\Delta_{mn}\right)\right]}, & k=1 \\ \sum_{i=1}^{j+l} -\frac{4C_{ki}\kappa}{\alpha_n\alpha_m} \frac{e^{-t_{oi}p}}{p\left[p+\kappa\left(\frac{60}{h^2}+\Delta_{mn}\right)\right]}, & k=2 \end{cases} \tag{23}$$

where

$$\Delta_{mn} = \alpha_n^2 + \alpha_m^2 = \left(\frac{n\pi}{a}\right)^2 + \left(\frac{m\pi}{b}\right)^2.$$

The inverse Laplace transformation and the inverse double Fourier finite-sine transformation give the final solution for the temperature field in the form

$$\tau_0 = \frac{16}{ab}\sum_{m=1,3,\ldots}^{\infty}\sum_{n=1,3,\ldots}^{\infty}\sum_{i=1}^{j+l}\left[C_{oi}\frac{1-e^{-\kappa\Delta_{mn}(t-t_{oi})}}{\alpha_n\alpha_m\Delta_{mn}}\right]H(t-t_{oi})\sin\alpha_n x_1\sin\alpha_m x_2$$

$$+\frac{4h^2}{3ab}\sum_{m=1,3,\ldots}^{\infty}\sum_{n=1,3,\ldots}^{\infty}\sum_{i=1}^{j+l}\left[C_{2i}\frac{1-e^{-\kappa\left(\Delta_{mn}+\frac{60}{h^2}\right)(t-t_{oi})}}{\alpha_n\alpha_m\left(\Delta_{mn}+\frac{60}{h^2}\right)}\right]H(t-t_{oi})\sin\alpha_n x_1\sin\alpha_m x_2,$$

$$\tau_1 = \frac{16}{ab}\sum_{m=1,3,\ldots}^{\infty}\sum_{n=1,3,\ldots}^{\infty}\left[\sum_{i=1}^{j}C_{1i}\frac{1-e^{-\kappa\left(\Delta_{mn}+\frac{12}{h^2}\right)(t-t_{oi})}}{\alpha_n\alpha_m\left(\Delta_{mn}+\frac{12}{h^2}\right)}-\sum_{i=1}^{l}C_{1i}\frac{1-e^{-\kappa\left(\Delta_{mn}+\frac{12}{h^2}\right)(t-t_{oi})}}{\alpha_n\alpha_m\left(\Delta_{mn}+\frac{12}{h^2}\right)}\right]H(t-t_{oi})\sin\alpha_n x_1\sin\alpha_m x_2, \quad (24)$$

$$\tau_2 = -\frac{16}{ab}\sum_{m=1,3,\ldots}^{\infty}\sum_{n=1,3,\ldots}^{\infty}\sum_{i=1}^{j+l}C_{2i}\frac{1-e^{-\kappa\left(\Delta_{mn}+\frac{60}{h^2}\right)(t-t_{oi})}}{\alpha_n\alpha_m\left(\Delta_{mn}+\frac{60}{h^2}\right)}H(t-t_{oi})\sin\alpha_n x_1\sin\alpha_m x_2.$$

5. Numerical example

Field amplitudes and current amplitudes decrease according to an exponential law $e^{\alpha x 3}$along the trajectory of wave propagation. The penetration constant is in accordance with the decay of one Neper (0.368) and its value is

$$\delta = \frac{1}{\alpha} = \frac{1}{\sqrt{\sigma\mu\pi f}}, \quad \left(\omega = \frac{2\pi}{T} = 2\pi f\right). \quad (25)$$

The skin depth δ decreases with the increase of frequency, conductivity and permeability.

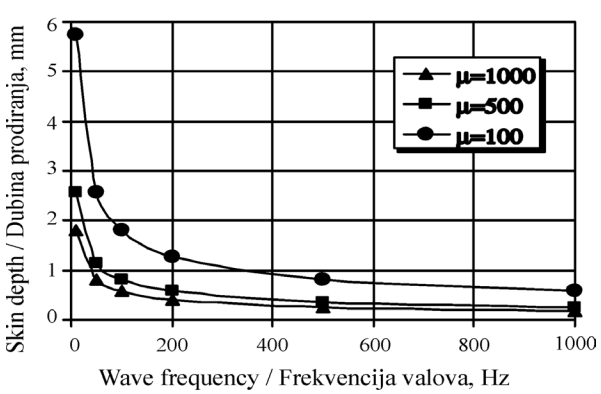

Figure 3. Skin depth as a function of wave frequency

Slika 3. Dubina prodiranja u funkciji frekvencije valova

Figure 3 shows variation of the skin depth as a function of wave frequency and relative magnetic permeability for a soft magnetic material. Electric conductivity of the material was 7.7×10^6 S/m.

For each ferromagnetic material mechanical, thermal and magnetic properties were obtained in a laboratory. As shown in [14], the magnetic and electrical properties of steel depends on a great number of factors such as the silicon and phosphorus content, ferrite grain diameter, sheet rolling method etc. The dependence of hysteresis losses on the ferrite grain diameter is shown in Figure 4 [14].

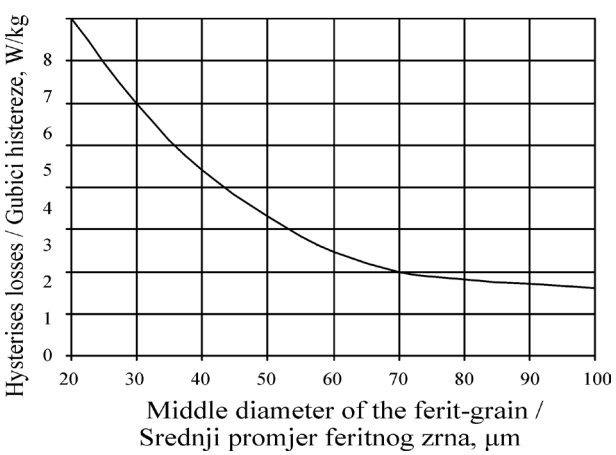

Figure 4. Hysterisis losses as a function of a ferrite-grain diameter

Slika 4. Gubici histereze u funkciji srednjeg promjera feritnog zrna

The temperature field shown in equations (3) and (24) corresponding to boundary conditions (19) is in the general case nonlinear along the plate thickness.

But in the case of very thin plates the temperature along the plate thickness is almost constant and can be approximated by the temperature in its middle plane

$$\theta(x_1, x_2, t) \approx \tau_0(x_1, x_2, t).$$

The first numerical example is given for a thin steel rectangular plate with dimensions: a=500mm, b=300mm and h=5mm. The plate was subjected to one

electromagnetic wave at the upper side with a magnetic intensity of H_0=5kA/m. The material properties regarding steel were: λ_o=50 W/mK, κ=1,4 10^{-3} m^2/s, μ_{rel}=500.

The diagram on Figure 5 represents the temperature in the middle point of the plate as a function of time and wave frequency. Under the influence of waves the plate heats up slowly and after about 40 minutes achieves the maximal temperature and moves to a stationary state.

Figure 6 shows the dynamic variation of the temperature in the middle point of the plate as a function of the plate thickness.

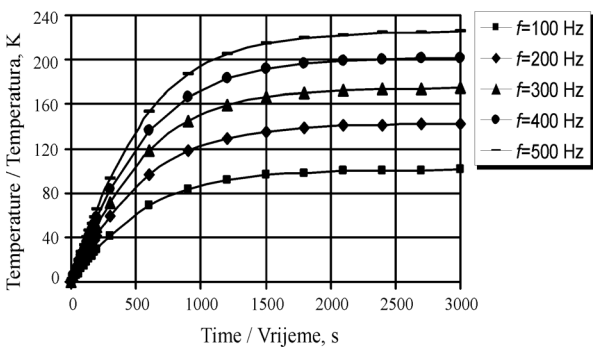

Figure 5. Temperature in the middle point as a function of time and wave frequency

Slika 5. Temperatura srednje točke ploče u funkciji vremena i frekvencije valova

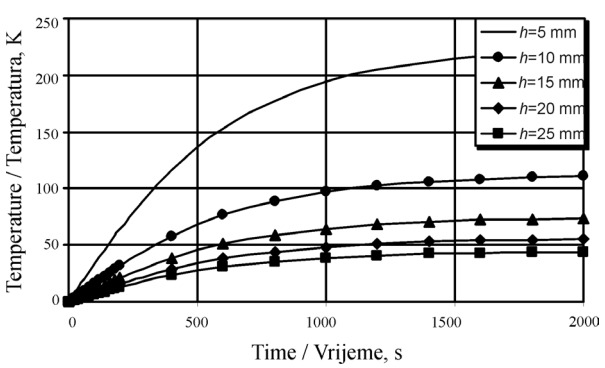

Figure 6. Temperature in the middle point as a function of time and plate thickness

Slika 6. Temperatura srednje točke ploče u funkciji vremena i debljine ploče

As a high frequency electromagnetic wave has a low skin depth, eddy-currents and hysterisis power losses act as a thermal load on the surface of the plate so increased plate thickness significantly lowers its temperature.

Figure 7 shows the temperature in the middle point subjected to an impulse electromagnetic wave. The wave is 5 kA/m strong and has a frequency of 500 Hz, while the impulse lasts 50 s, and the time between two neighboring impulses (relaxation time) is 100 s.

Mechanical behaviour of the plate was obtained according to Finite element analysis. Based on the analytical solution (24), a program for obtaining temperature in the nodes was made to be adjustable to the FEM Program package KOMIPS [15]. The temperature field obtained using analytical solution for t =100 s is presented on Figure 8a.

Figure 8b represents stress fields in the plate for two types of boundary conditions: supports on two subtended edges and supports on the entire edge. The equivalent stress was obtained using the Huber-Hencky-Mises hypothesis.

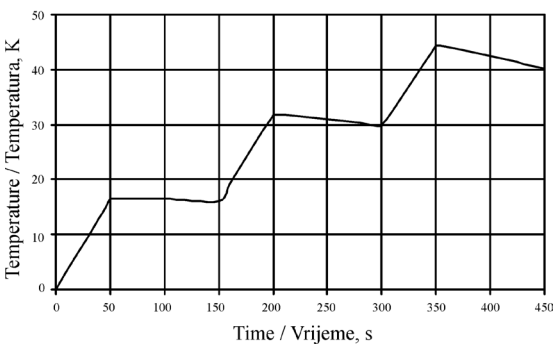

Figure 7. Temperature in the middle point subjected to an impulse electromagnetic wave

Slika 7. Temperatura srednje točke ploče pod djelovanjem impulsnog elektromagnetskog vala

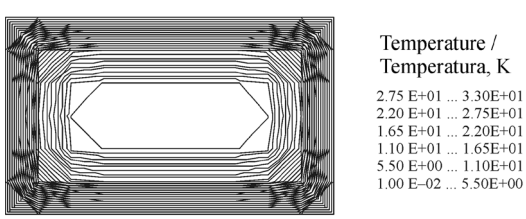

Figure 8a. Temperature in the middle surface after 100 s

Slika 8a. Temperatura srednje ravnine poslije 100 s

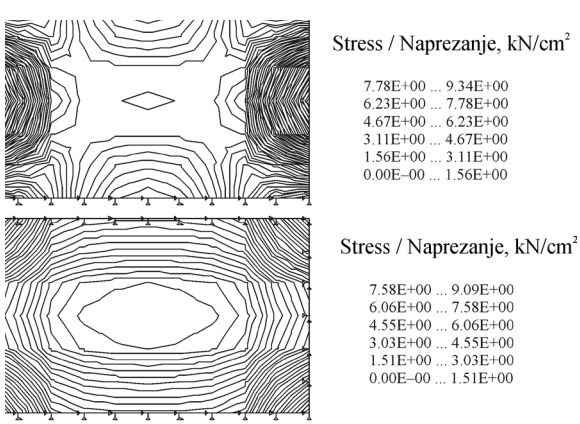

Figure 8b. Stress fields in the middle surface after 100 s for two types of boundary conditions

Slika 8b. Polje naprezanja u srednjoj ravnini ploče poslije 100 s za dvije vrste rubnih uvjeta

Appropriate results for the stationary state (after about half an hour) are presented on Figure 9.

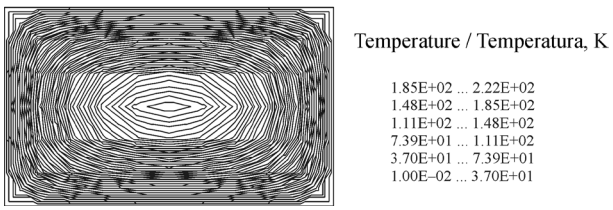

Figure 9a. Temperature in the middle surface after 2000 s

Slika 9a. Temperatura srednje ravnine poslije 2000 s

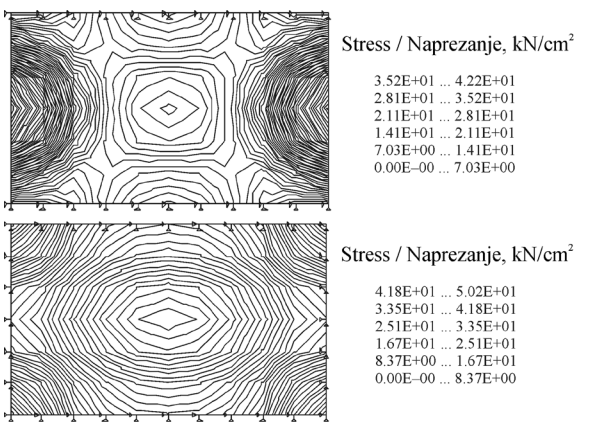

Figure 9b. Stress fields in the middle surface after 2000 s for two types of boundary conditions

Slika 9b. Polje naprezanja u srednjoj ravnini ploče poslije 2000 s za dvije vrste graničnih uvjeta

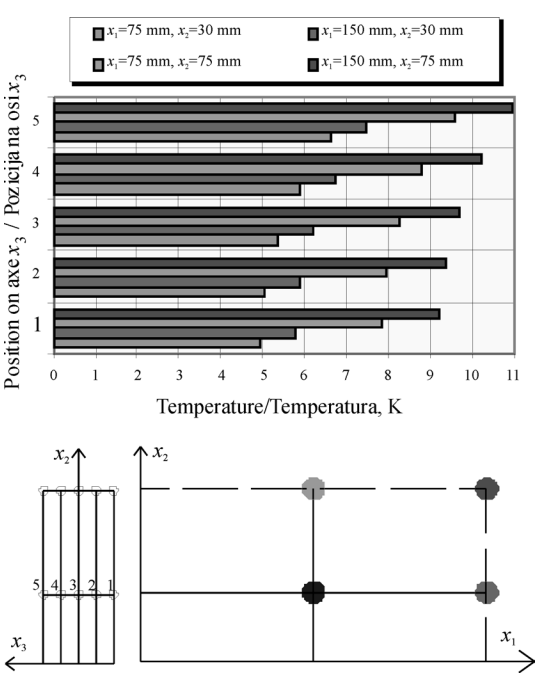

Figure 10. Temperature distribution across the plate thickness after 500 s

Slika 10. Raspodjela temperature po debljini ploče poslije 500 s

In the case of thick plates the temperature must be approximated using all three components - τ_o, τ_1 and τ_2

$$\theta(x_1,x_2,x_3,t)=\tau_0(x_1,x_2,t)+x_3\tau_1(x_1,x_2,t)+x_3^2\tau_2(x_1,x_2,t).$$

The following example presents the behaviour of a thick steel rectangular plate with dimensions a=300 mm, b=150 mm and h=30 mm. The material properties are the same as in the previous example.

As the plate has symmetry properties, the temperature distribution across the plate thickness was calculated for one quarter of the plate and for five positions on the axis x_3 (according to Figure 10): Pos.1 x_3 = -15 mm, Pos. 2 x_3 = -7.5 mm, Pos. 3 x_3 = 0 mm, Pos. 4 x_3 = +7.5 mm and Pos. 5 x_3 = +15 mm.

Appropriate results for four different values of the coordinates x_1 and x_2 are presented in Figure 10.

According to the previous conclusion, a 3D volume finite element model was formed and the thick plate was loaded with the analytically calculated temperature field presented in Figure 11a.

Deformation and stress were calculated using FEM analysis for the case of supports on two longer subtended edges (Figure 11b and 11c).

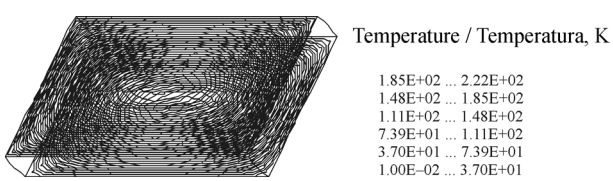

Figure 11a. Temperature in the plate after 500 s

Slika 11a. Temperatura ploče poslije 500 s

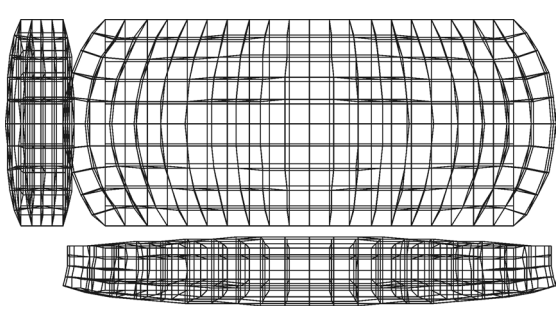

Figure 11b. Deformation of the plate after 500 s

Slika 11b. Deformacija ploče poslije 500 s

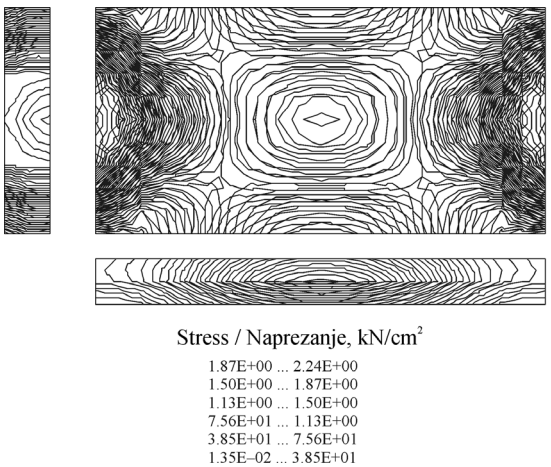

Figure 11c. Equivalent stress after 500 s

Slika 11c. Ekvivalentno naprezanje poslije 500 s

6. Conclusions

The problem of a metallic plate subjected transversally to the line of propagation of simple harmonic electromagnetic waves can be described through three systems of differential equations: Maxwell's equations, equations governing the temperature field and equations describing deformation and stress fields. In the case of high frequency waves the temperature increase has the greatest influence on the stress field. That is the result of a time changing field (appearance of eddy-current losses and hysterisis losses). The intensity of the losses is of an exponential type across the thickness of the plate, so distribution of the temperature across the plate thickness has to be obtained in a nonlinear form. The temperature field increases with the increase of wave frequency, hysterisis factor and decrease of the plate thickness.

A very suitable method for solving the presented problem in an analytical form, as shown in this paper, is the integral transform technique. For dynamic and geometrically complicated problems with non homogeneous boundary conditions it is very difficult to find vibrations and stress in an analytical form. So, involving the finite element method in calculation is preferable. Depending on the skin depth and plate thickness a suitable approximation level of the analytical solution is adopted. In accordance with this the problem is modeled using surface or volume finite elements..

REFERENCES

[1] PAO, Y.H.; YEH, C.S.: *A Linear Theory for Soft Ferromagnetic Elastic Solids*, Int. J. Enging. Sci., 11 (1973) 415-436.

[2] MOON, F. C.; PAO, Y. W.: *Magnetoelastic Buckling of a Thin Plate*, Journal of Applied Mech., 35, Trans. ASME, Ser. E (1968) 53-58.

[3] SHINDO, Y.: *Dynamic Singular Stresses for a Griffith Crack in a Soft Ferromagnetic Elastic Solid Subjected to a Uniform Magnetic Field*, Journal of Applied Mech., 50, Trans. ASME, Ser. E (1983) 50-56.

[4] CHOUDHURI, S.K.; DEBNATH, L.: *Magnetoelastic Plane Waves in Infinite Rotating Media*, Journal of Applied Mech., 50, Trans. ASME, Ser. E (1983) 283-287.

[5] ROYCHOUDHURY, S.K.; BANERJEE, M.: *Magnetoelastic plane waves in rotating media in thermoelasticity of type II*, IJMMS, 71 (2004) 3917-3929.

[6] PARKUS, H.: *Electromagnetic Interactions in Elastic Solids*, Springer-Verlag (1979)

[7] KRAKOWSKI, M.: *Mathematical Model of Eddy Currents in a Metallic Solid after Applying an External Magnetic Field*, Bullet. of the Polish Acad. of Science, 29, No. 5-6, Warsaw (1981) 67-71.

[8] PEACH, M.O.; CHRISTOPHERSON, N.S.; DALRYMPLE, J.M.; VIEGELAHN, G. L.: *Magnetoelastic Buckling: Why Theory and Experiment Disagree*, Experimental Mech., 28, No 1 (1988) 65-69.

[9] SHEN, H.; YAO, Z.Q.; SHI, Y.J.; HU, J.: *Study on temperature field in high frequency induction heating,* Acta. Metall. Sin. 19, No. 3 (2006) 190-196.

[10] KRAKOVSKII, V. A.: *High-temperature superconducting microstrip transmission lines,* Russ. Physics Jour. 45, No. 10 (2002) 955-961.

[11] MILOŠEVIĆ, MITIĆ V.: *Magneto-thermo-elastic bending of thin plates*; Monogr., Zadužbina Andrejević, Belgrade (1999).

[12] MILOŠEVIĆ MITIĆ, V.; MANESKI, T.: *The Influence of the Nonlinear Temperature Field on the Behavior of the Metallic Plate Induced by Two Electromagnetic Waves Obtained by GSP*, Facta Univers., Ser. Mech., Auto. Control and Robotics, 3, No 15 (2003) 1113 – 1120.

[13] MILOŠEVIĆ, V.: *Temperature, Strain and Stress Fields Produced by Impulsiv Electro-magnetic Radiation in the Thin Metallic Plate*, XIXth ICTAM, Kyoto, Japan (1996).

[14] GOGER, M.; MANŽUROV, D.: *Činitelji od utjecaja na tehnološka i elektromagnetska svojstva čeličnih limova primjenljivih za izradu magnetskoga kruga elektromotora*, Strojarstvo, Zagreb 18 (1976) 6, 313-323.

[15] ZLOKOVIĆ, G. M.; MANESKI, T.; NESTOROVIĆ, M.: *Group Supermatrix Procedure in Computing of Engineering Structures,* Structural Engineering Review, 6, No 1 (1994).